Differential Ionic Permeation of DNA-Modified Electrodes

Donato M. Ceres,[†] Andrew K. Udit,[‡] Haley D. Hill,[‡] Michael G. Hill,*[,‡] and Jacqueline K. Barton*[,†]

Division of Chemistry and Chemical Engineering, California Institute of Technology, Pasadena, California 91125, and Department of Chemistry, Occidental College, Los Angeles, California 90041

Received: September 26, 2006; In Final Form: November 10, 2006

Ionic permselectivity of DNA films has been investigated by the analysis of the electrochemical response of methylene blue (MB) as a function of pH and ionic strength on DNA-modified electrodes in aqueous *p*-nitrophenol (*p*-NP) and phosphate buffers. We have observed a linear Pourbaix diagram in *p*-NP buffer indicating that the reduction of MB occurs with a two-electron plus one-proton reaction. Interestingly, in phosphate buffer the Pourbaix diagram is curved and this suggests that the thermodynamics of MB incorporated in the film depend also on the ratio of mono- versus divalent anions in the bulk. This result indicates that DNA films do not behave as pure ion-exclusion films, but instead there is a differential permselectivity that depends on the identity of the anions. Based on this consideration of the ionic distribution in the films, we provide a new method for the analysis of the DNA surface coverage based on AC impedance of an anionic species, ferricyanide. The methodology is of particular value in analyzing DNA hybridization and dehybridization. This approach presents an advantage compared to standard ruthenium hexammine assays since our methodology is insensitive to film morphology, and is highly sensitive to the amount of negative charge on the surface.

Introduction

DNA-modified electrodes offer a unique platform for investigating charge transport (CT) through the double helix[1−7] and have been increasingly employed for the development of DNA diagnostics[8,9] and the study of nucleic acid−protein interactions.[10−13] Many of these applications rely on redox-active small molecules that bind to DNA via electrostatics and/or intercalation, and the extent of that binding depends on ionic strength, concentration, and the surface structure of the DNA film. Indeed, the film morphology itself is highly dependent on specific solution conditions, and both single- and double-stranded DNA coatings can be self-assembled onto metal surfaces with control of coverage and spacing between the individual molecules.

All of these properties derive ultimately from interfacial interactions of the highly charged polyanionic sugar−phosphate backbone with the surrounding electrolyte solution. Indeed, that nucleic acids (e.g., ∼15−20 base-pair duplexes) can essentially close pack upright on gold is remarkable: at a concentration of ∼40 pmol/cm^2 (coverages reported based up ^{32}P-labeling studies)[3] the interhelical spacing is only ∼6 Å. Notably, preparing films with this level of DNA loading requires a high concentration of divalent cations (usually Mg^{2+}) during the self-assembly process, conditions similar to those used to crystallize DNA.[14,15]

One result of such a high concentration of immobilized negative charges is the potential for DNA films to function as cation-exchange membranes. Restricted transfer of ions across a film−solution interface can have profound effects on the thermodynamics and electron-transfer kinetics of redox molecules within the film.[16] Given the practical applications of DNA electrodes in biosensing and analysis, it is critical to understand how the ionic distribution associated with charge neutrality within the DNA films is established, and to what extent that distribution can affect the interpretation of electrochemical data. More fundamentally, investigating the differential permeation of ionic species (permselectivity) of DNA-modified electrodes can provide insight into the structure of the film itself, and by extension, the ability of DNA to mediate charge transport.

The general phenomenon of DNA condensation has been investigated extensively.[17−20] DNA packing is greatly facilitated by the presence of divalent cations (e.g., Mg^{2+}), where it is believed that overscreening of the phosphate backbone leads to charge inversion, followed by attraction of adjacent DNA helices.[21−24] Indeed, two-dimensional condensation of DNA chains has been observed[25−27] at cationic membranes by the simple addition of Ca^{2+}, Mg^{2+}, or Mn^{2+} ions, and we have found that high concentrations (∼0.1 M) of $MgCl_2$ are necessary for the self-assembly of tightly packed duplex DNA films on gold. Notably, we observe no DNA precipitation from the bulk solution under our deposition conditions; this finding suggests a "liquid-crystal"-like description of the DNA SAM, where the individual helices are confined to a two-dimensional array via the gold−thiol linkage.

The distribution of ions within the DNA film is likely quite complicated, where both di- and monovalent ions and ion-pairs may coexist. Removing the film from the deposition solution and placing it in Mg^{2+}-free buffer is an additional perturbation, as a new ionic equilibrium must be established to maintain charge neutrality. Regardless of the exact composition of this equilibrium, however, the presence of immobilized phosphate groups within the polyelectrolyte induces a Donnan potential (E_D, Figure 1) across the film/solution junction, owing to the unequal distribution of diffusible ions between the two phases.

* Address correspondence to this author. E-mail: mgh@oxy.edu (M.G.H.) and jkbarton@caltech.edu (J.K.B.).
[†] California Institute of Technology.
[‡] Occidental College.

10.1021/jp066324c CCC: $37.00
Published on Web 01/03/2007

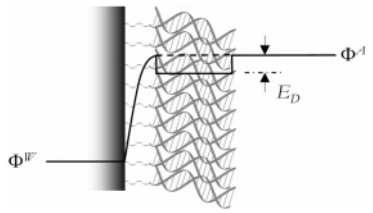

Figure 1. Idealized electrostatic-potential profile for a DNA film assuming complete permeation of the DNA film, showing a Donnan potential (E_D) at the film/solution junction as the result of an unequal distribution of diffusible ions across the interface.

As the junction is largely impermeable to at least one of the ions present, the magnitude of the E_D is directly related to the bulk concentration of supporting electrolyte.

As originally noted by Anson for nafion coatings,[16] if the film is sufficiently permselective, electrochemical reduction of a positively charged species within the monolayer must be accompanied by penetration of a cation from the supporting electrolyte (C_S^+) into the film. In general, changes in both ionic strength and pH can modulate the formal potential of a redox species incorporated into a DNA film according to eq 1,

$$E_{1/2}^{app} = E^{0\prime} + \frac{RT}{F}\frac{(n-m)}{n}\ln\left(\frac{[C_S^+]}{[C_f^+]}\right) + \frac{RT}{F}\frac{m}{n}\ln[H^+] \quad (1)$$

where the half-reaction describing an n electron/m protons (ne^-/mH^+) reduction is given by

$$Ox^{b+} + (n-m)C_S^+ + ne^- + mH^+ \leftrightarrow [Red{\cdot}H_m]^{(b-n+m)+} + (n-m)C_f^+ \quad (2)$$

As a result, $E_{1/2}^{app}$ is expected to change by $(n-m)/n{\cdot}59$ mV (at 25 °C) for every 10-fold change in C_S^+ and by $m/n{\cdot}59$ mV for every pH unit. Measuring the characteristic pH and ionic-strength dependences of a formal redox couple embedded within the film therefore provides a convenient assay for determining parameters such as the number of electrons n, protons m, and the pK_a of molecules bound to DNA, especially where coulometric data are ambiguous.

Here we describe the pH and ionic-strength dependence of the methylene blue/leucomethylene blue (MB/LB) redox couple intercalated into DNA films. We additionally present electrochemical data using purely electrostatic redox reporters such as $Ru(NH_3)_6^{3+}$ and $Fe(CN)_6^{3-}$. These data support fully the idea that DNA films exhibit highly selective, though not complete, ionic permeation, and provide the basis for simple experimental methods to characterize (e.g., determine the number of electrons/protons transferred, measure pK_a, etc.) and fine-tune the potentials of electrochemical reactions for molecules bound to DNA. They also suggest a simple assay based on electrochemical impedance spectroscopy for DNA-film composition that does not rely on specific (and potentially complicated) electrostatic interactions between DNA and cationic reporter molecules.

Experimental Section

DNA Film Self-Assembly. Oligonucleotides (sequence: 5′-AGT ACT GCA GTA GCG-3′) were disulfide modified at the 5′-hydroxy terminus according to procedures previously reported.[1] Sequences were purified by reverse-phase HPLC, converted to free thiols with dithiothreitol, and repurified before hybridization to their complements. Next, 10 μL of a 50 μM dsDNA/0.1 M $MgCl_2$ solution were deposited onto gold electrodes (area ~0.02 cm^2) that had been freshly polished (0.05 μm alumina) and electrochemically etched (1 M H_2SO_4). After 12 h, the modified electrodes were thoroughly rinsed in Mg-free phosphate buffer (5 mM phosphate, 50 mM NaCl) and immediately used for electrochemical analysis. For experiments involving mixed DNA/mercaptohexanol (MCH) monolayers, electrodes were prepared by depositing 50 μM thiolated dsDNA on gold for 1 to 2 h with no $MgCl_2$ present. After rinsing in phosphate buffer, the electrodes were incubated in a solution of 1 mM MCH/50 mM phosphate buffer with 1% v:v ethanol (pH 7.0) for approximately 1 h. Electrodes were routinely assayed for surface coverage with both Tarlov's $Ru(NH_3)_6^{3+}$ electrochemical assay[28] and AC impedance measurements (vide infra). The 5 mM sodium phosphate and *p*-nitrophenol buffers used for all experiments were treated with NaCl to achieve the desired ionic strength, and adjusted to their proper pH with NaOH and HCl.

DNA Dehybridization/Rehybridization. Duplex-modified DNA films were dehybridized by incubating the electrodes at 64 °C in 10 mM Tris-HCl, pH 8.0 (dehybridization buffer, DHB). Rehybridization was accomplished by re-incubating the modified electrode in 50 mM sodium phosphate buffer, pH 7.0 containing 1 μM ssDNA at ambient temperature (rehybridization buffer, RHB).

Electrochemistry. All electrochemical measurements were performed with a 760B biopotentiostat (CH Instruments) in a conventional three-compartment electrochemical cell. A platinum wire (Alfa) served as the auxiliary electrode, and a SCE was used for the reference. The reference compartment was separated from the working compartment by a modified Luggin capillary. All potentials are reported versus SCE.

Results and Discussion

Electrochemistry of MB at DNA-Modified Electrodes. To test the validity of eq 1, we have investigated the electrochemistry of the DNA-intercalator methylene blue (MB) as a function of pH and ionic strength. As previously demonstrated, MB binds strongly and reversibly to duplex DNA films, exhibiting a reversible, proton-coupled reduction.[3−5] These DNA films are furthermore routinely characterized, as described earlier, to establish the integrity of the film containing closely packed DNA duplexes with no pinholes. At the concentration of 2 μM (a concentration below the surface saturation of about 5−6 μM), MB surface density is always between 20 and 30 pmol/cm^2 indicating that it cannot penetrate the film. The presence of pinholes would result in multiple MB molecules bound per DNA duplexe and thus in a much higher electrochemical response. Importantly, MB exhibits Langmuir binding with on and off rates of 3×10^4 M^{-1} s^{-1} and 0.043 s^{-1},[29] respectively.

Figure 2 shows the cyclic voltammetry of 2 μM MB in 50 mM sodium *p*-nitrophenol buffer, Na^+/*p*-NP (pK_a *p*-NP = 6.5), over the pH range 5.5−8.5; a plot of the resulting values of $E_{1/2}^{app}$ vs pH is given in Figure 3a. The apparent formal potential shifts a nearly ideal 30 mV/pH unit, consistent with a $2e^-/H^+$ redox couple over the entire pH range.

Equation 1 additionally predicts a 30 mV/decade change in $[C_S^+]$ for a $2e^-/H^+$ process. Figure 3b shows the formal potential of MB plotted against the bulk concentration of Na^+ for Na^+/*p*-NP buffers prepared at pH 6.5. As expected, the potential change is approximately 30 mV/decade confirming the $2e^-/H^+$ nature of the MB/LB redox couple. Together, these pH and ionic-strength dependencies validate the use of eq 1, and suggest a high degree of permselectivity at the DNA-film/solution interface.

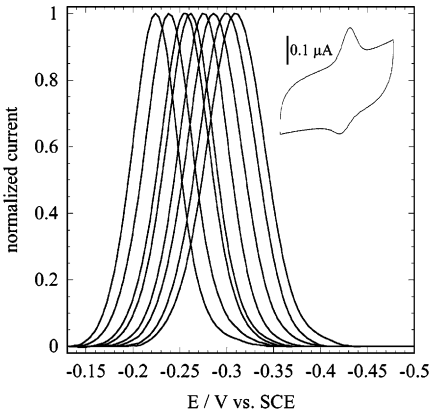

Figure 2. Normalized, background-subtracted cathodic peak of MB in *p*-NP buffer at pHs (form left to right) 5.5, 6.0, 6.5, 6.7, 7.2, 7.5, 8.0, and 8.5. The inset shows a typical cyclic voltammogram of 2 μM MB at a DNA-modified electrode obtained in *p*-NP pH 7.2, at 100 mV/s from 0 to −450 mV versus SCE.

Interestingly, the situation in phosphate buffer is not as straightforward. Figure 4 shows the pH dependence of $E_{1/2}^{app}$ for MB in solutions containing 5 mM phosphate buffer/0.1 M NaCl (under these conditions the ionic strength of the solution does not change appreciably with pH); unlike the results for the Na^+/*p*-NP system, here the plot is uniformly curved over the entire pH range. A possible explanation for this apparent anomaly is differential permeation of mono- and divalent phosphate ions within the DNA films. Because the relative concentration of mono- vs divalent phosphate in the film is a function of the pH in the bulk of the solution, the total concentration of film-bound cations ($[C_f^+]$, eq 1) changes as well, affecting the Donnan potential E_D. Notably, reversing eq 1 and plotting $[C_f^+]$ as a function of pH (using $E^{0\prime} = -0.058$ V obtained from the intercept of the linear fit in Figure 3a) reveals a variation of $[C_f^+]$ within the film that maximizes at the pK_a of $H_2PO_4^-$ (pK_a = 6.8, Figure 4b), where the concentrations of mono- and divalent anions are equal. This suggests the existence of a direct relationship between $[C_f^+]$ and the ratio $H_2PO_4^-$/ HPO_4^{2-}; indeed, at pH 6.8 we find a slope of 30 mV per pH unit, where the influence of the variation of $[C_f^+]$ is minimal.

Qualitatively, Figure 5 shows a comparison between the cyclic voltammograms of MB obtained in phosphate and *p*-NP buffers under similar ionic strengths. The change in background capacitance is a clear indication that the two electrolytes interact with the film in different ways.

Implications for the Electrochemical Behavior of Highly Charged Redox Species at DNA Films. Tarlov and co-workers have developed an electrochemical assay for DNA surface coverage based on $Ru(NH_3)_6^{3+}$, where the coulometry of the $Ru^{3+/2+}$ couple is directly proportional to the number of phosphates in the DNA backbone.[28] Indeed, $Ru(NH_3)_6^{3+}$ has been utilized frequently for electrochemical quantitation of oligonucleotides on surfaces, and the assay has been extended to measure the electrostatic binding constants of non-redox-active cations to DNA via competitive binding experiments. That $Ru(NH_3)_6^{3+}$ binds strongly to DNA electrodes is evident in the cyclic voltammetric response that resembles that of a surface-bound species, where the peak shape is symmetric and lacks a diffusive tail (Figure 6). Importantly, in the absence of competitive counterions (such as Na^+), $Ru(NH_3)_6^{3+}$ must also serve to maintain charge neutrality during a redox reaction described by eq 2, so its electrochemical response (thermodynamics and kinetics) is expected to be highly dependent on the structure and ionic composition of the film.[30,31]

To illustrate this effect, the cyclic voltammogram of 5 μM $Ru(NH_3)_6^{3+}$ at a DNA film (~10 pmol/cm^2) in the absence of competing Na^+ is shown in Figure 6. The cyclic voltammogram clearly is not stable upon multiple cycling, and the integrated signal (and hence the supposed surface concentration of DNA) varies considerably depending on the number of scans. Moreover, the nonlinear pH dependence of $E^{0\prime}$ in phosphate buffer is strong evidence that the identity and concentration of anions (e.g., mono- versus divalent) in the supporting electrolyte can affect the differential ionic selectivity of the film, thus the concentration of redox-active cations may not be strictly proportional to the number of immobilized DNA backbone phosphates.

A complementary electrochemical method for determining surface coverage would be valuable. This need for a new method of determining surface coverages is particularly relevant when assaying for changes in the structure of the DNA film itself, for instance when monitoring DNA hybridization: cation permeation into the film depends not only on concentration and specific electrolyte conditions, but also on the density and distribution of immobilized charges within the DNA coating.

Hybridization Assay for DNA Films Based on AC Impedance. As an alternative, we have found that long-range electrostatic repulsion of the highly charged anionic complex $Fe(CN)_6^{3-}$ is much less sensitive to film morphology and specific buffer conditions, making it an excellent electrochemical reporter for hybridization at DNA surfaces. Cyclic voltammo-

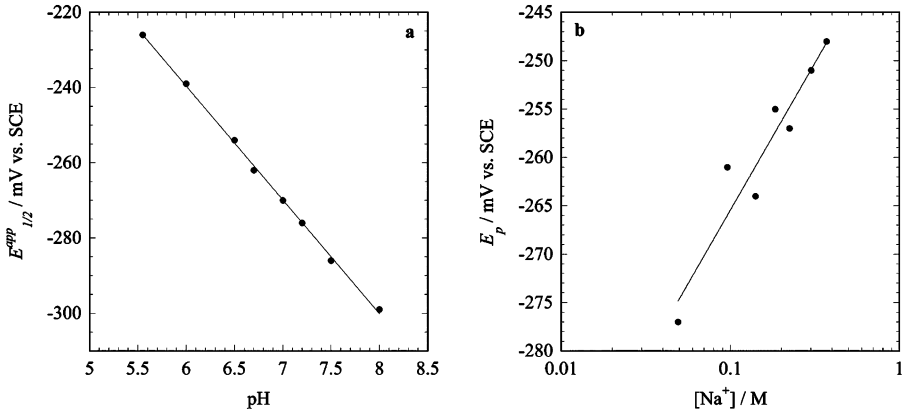

Figure 3. (a) Pourbaix diagram for MB on a DNA-modified gold electrode in *p*-NP buffer. The solid line is the linear fit with slope of 30.3 mV per pH unit ($R = 0.999$). (b) Ionic strength dependence of MB reduction in *p*-NP buffer at a DNA-modified gold electrode obtained at pH 7.2. The solid line is the logarithmic fit a log[Na^+] with $a = 30.4$ mV per decade ($R = 0.954$).

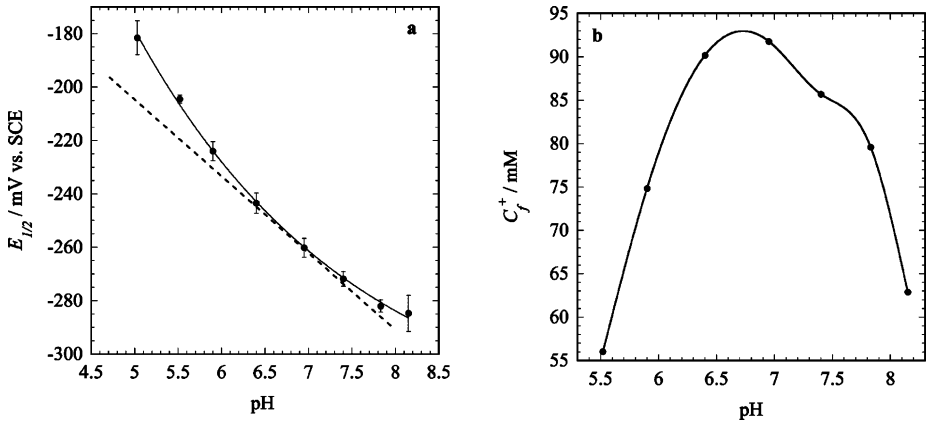

Figure 4. (a) Pourbaix diagram for MB on a DNA-modified gold electrode in the presence of phosphate buffer. Error bars represent the standard deviation over three independent trials. The solid line serves as a visual guide for showing better the nonlinear character of the plot. The dotted line represents the tangent of the curve at pH 6.8, with a 30 mV/decade slope. (b) Variation of the counterion concentration inside the DNA film as a function of the pH obtained from eq 1. The solid line serves as a visual guide.

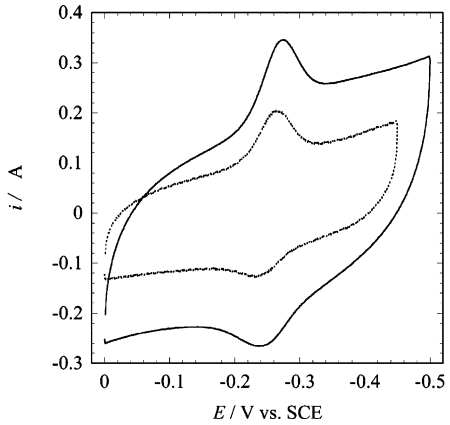

Figure 5. Typical cyclic voltammogram of 2 μM MB at a DNA-modified gold electrode in 5 mM phosphate buffer, 100 mM NaCl (solid line) and 5 mM *p*-NP buffer, 200 mM NaCl (dashed line) both at pH 7.0 and 100 mV/s.

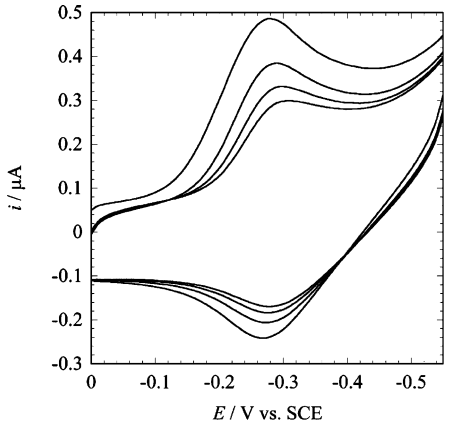

Figure 6. Cyclic voltammogram of 5 μM $Ru(NH_3)_6^{3+}$ in 10 mM Tris-HCl, pH 8.0, on a loosely packed DNA film. The integrated peak charges at each cycle are 220, 150, 100, 80 nC, a variation of about 65%.

grams (CVs) of $Fe(CN)_6^{3-}$ at well-packed DNA films are featureless, indicating that $Fe(CN)_6^{3-}$ is effectively blocked from the surface. At more loosely packed films ($\Gamma_{DNA} < \sim 10$ pmol/cm^2) the CVs exhibit features that suggest either sluggish kinetics or access to the electrode surface through pinholes. In the former case, peak splitting can be extremely large and often shifts the anodic peak potential well beyond the solvent limit; alternatively, penetration of $Fe(CN)_6^{3-}$ through pinholes is characterized by an "S" shape voltammogram indicating radial diffusion to an active surface of just a few microns in diameter.

While instructive qualitatively, neither CV response yields quantitative data regarding film composition. We therefore turned to electrochemical impedance spectroscopy (EIS) to provide a clearer picture of the interaction of $Fe(CN)_6^{3-}$ at DNA-modified electrodes. In the EIS experiment, a small oscillating potential is applied at the formal redox potential of the reporter molecule and the impedance is measured over a frequency spectrum, e.g., $0.1-10^5$ Hz. A plot of the impedance in the complex plane (Nyquist plot) shows a semi-arc at high frequency yielding information about capacitive processes, and a 45° line at low frequencies representing slower events such as mass transfer.[32] In the context of the simplified Randles equivalent circuit, the diameter of the impedance arc (on the real axis of the impedance) is related to the electron-transfer resistance, R_{ET}, which, in turn, can be related to the extent of electrode passivation. In the particular case of DNA-modified electrodes, the degree to which $Fe(CN)_6^{3-}$ penetrates the film is reflected in R_{ET}, thus providing a quantitative measure of the relative DNA surface coverage.

To illustrate the sensitivity of the EIS technique we investigated the heat denaturation and rehybridization of DNA at mixed DNA/mercaptohexanol (MCH) electrodes. Because alkane−thiol monolayers readily undergo surface reorganization upon heating we first examined the electrochemical response of $Fe(CN)_6^{3-}$ at MCH films in the absence of DNA. Although the ferri/ferrocyanide redox reaction is often sluggish at metallic surfaces, the CV response at gold/MCH shows rapid electron-transfer kinetics (dashed line, Figure 7). Upon heating (64 °C) and cooling back down to ambient temperature, the response becomes even more reversible (solid line, Figure 7) and is essentially ideal at 50 mV/s (digital simulations over a range of scan rates yield a standard ET rate, $k°$, of 0.013 s^{-1} cm^{-2}). Notably, this apparent film reorganization has a dramatic effect on the EIS response: after one heating cycle the R_{ET} nearly vanishes (or at least is less than the solution resistance) and the redox reaction is governed mainly by mass transport (Figure 8).

Incubation of an MCH film in solutions containing single-stranded DNA (ssDNA) does not affect the impedance response of $Fe(CN)_6^{3-}$, suggesting that ssDNA does not adsorb on the film to any appreciable degree (dashed and dotted lines are indeed overlapping in Figure 8). Thus, MCH films provide a biocompatible surface for DNA that does not induce ferricyanide

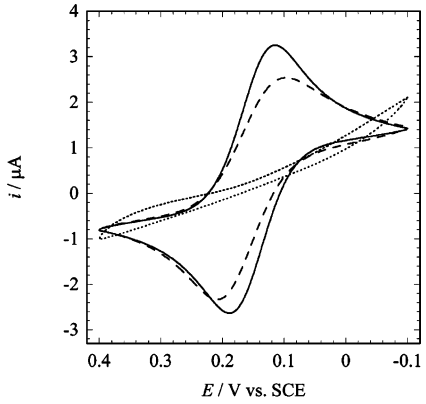

Figure 7. Cyclic voltammogram of $Fe(CN)_6^{3-}$ on a MCH-modified electrode before (dashed line) and after heat treatment in Tris buffer at 64 °C (solid line). The dotted line is the electrochemical response of $Fe(CN)_6^{3-}$ on a DNA-MCH mixed monolayer. Conditions: 50 mM phosphate buffer, pH 7.0, 1 mM $Fe(CN)_6^{3-}$, 50 mV/s.

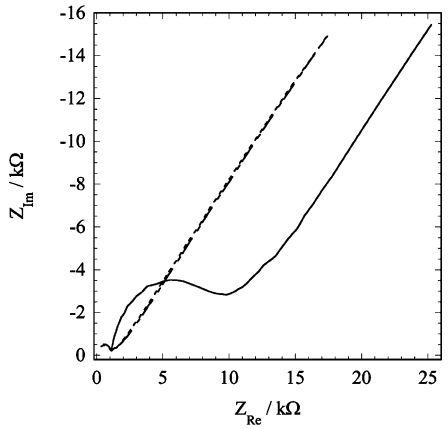

Figure 8. Nyquist plot for $Fe(CN)_6^{3-}$ on a fresh MCH-modified electrode (solid line), after heat treatment (dot-dashed line), and after incubation with 1 μM ssDNA for 20 min at room temperature (dotted line). Both broken curves are perfectly overlapping.

adsorption, nor does MCH backfilling appear to affect the affinity of small molecules or proteins to surface-bound DNA.

In contrast to the response of ferricyanide at MCH-modified surfaces, the CV of $Fe(CN)_6^{3-}$ at a mixed DNA/MCH monolayer suggests a well passivated surface (dotted curve in Figure 7). The absence of a linear slope at low frequencies in the impedance response provides additional evidence for the lack of mass transport to the surface. Figure 9 shows the impedance responses for several cycles of hybridization and dehybridization. The solid-line curve with filled dots (numbered 1 in Figure 9) represents the impedance response of a freshly prepared electrode, after thorough rinsing in a dehybridization buffer (DHB, see Experimental Details) at room temperature. A slight increase of R_{ET} is observed after incubation of the electrode in the same buffer at 37 °C (a temperature that is below the melting temperature of the DNA) for about 20 min (solid line, 2). This indicates that rinsing and slight heating in dehybridization buffer, which lacks Na^+, might have slightly decreased the ionic strength in the film, decreasing the Debye screening and resulting in a greater repulsion for $Fe(CN)_6^{3-}$. Only after incubation of the electrode in hot (64 °C) dehybridization buffer does the DNA begin to dehybridize, as is evident by the decrease of R_{ET}. Indeed, R_{ET} decreases as a function of time, approaching a lower limit at ~20 min, at which point only ssDNA remains on the surface. Incubation of the electrode in a rehybridization buffer (RHB, see the Experimental Section) for 15 min at

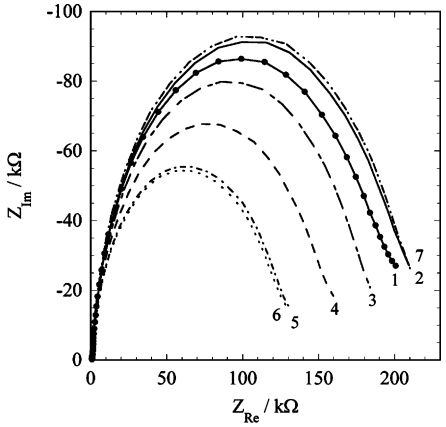

Figure 9. Nyquist plots for $Fe(CN)_6^{3-}$ on a DNA-modified electrode backfilled with MCH for a series of dehybridization and rehybridization times: fresh electrode (solid-filled circles, 1), after heating at 37 °C for 45 min in DHB (solid, 2), after dehybridization for 7 min (dash-line, 3), after an additional 5 min dehybridization (line-line, 4), and for 33 min (dot-line, 5) and 10 min more (dotted, 6), and rehybridization for 15 min with complementary strand (dot-dot-line, 7). Dehybridization was performed by incubation of the electrode in the DHB at 64 °C, while rehybridization was done by incubating the electrode in RHB containing 1 μM complementary DNA at room temperature.

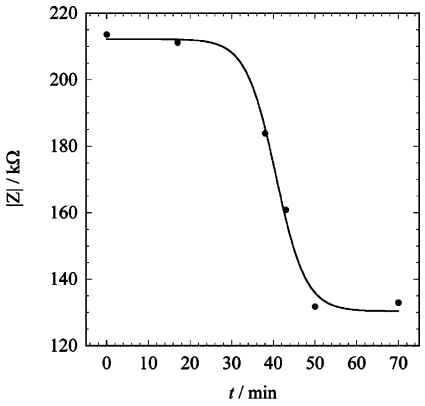

Figure 10. Plot of the module of the impedance at low frequency as a function of the incubation time for the dehybridization of the complementary DNA strand on a DNA film.

ambient temperature brings R_{ET} back nearly to its original value. After incubation for an additional 15 min, the impedance response of the film is indistinguishable from its original shape. A plot of the module of the impedance for various incubation times is shown in Figure 10, suggesting that melting/hybridization is cooperative at these electrodes.

From these experiments we conclude that it is possible to fully dehybridize then rehybridize surface-bound DNA under these conditions. That we have carried out such cycles multiple times on the same sample demonstrates the robust nature of the DNA film. Significantly, rehybridization utilizing a non-complementary sequence has essentially no effect on the impedance response, supporting our assertion that observed changes are due to actual hybridization and not nonspecific adsorption (Figure 11).

Conclusion

DNA films are polyelectrolytes and the interfacial properties of DNA-modified electrodes cannot be understood fully without taking into account this ionic character. Because electrostatic interactions between individual DNA molecules within the film determine the extent of permselectivity for both cations and anions, Donnan potentials across the interface are highly

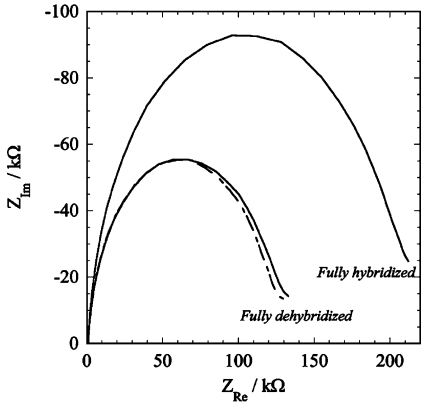

Figure 11. Nyquist plots for $Fe(CN)_6^{3-}$ on a DNA-modified electrode backfilled with MCH. The two solid line curves represent the cases where the film is fully dehybridized (small impedance) or fully hybridized (high impedance). Rehybridization for 20 min in the conditions of Figure 9 with noncomplementary DNA does not change appreciably the impedance of the surface (dash-line curve).

sensitive to packing, solution ionic strength, and the identity of the electrolyte. Indeed, the extent of the permselectivity is apparently related to the initial deposition conditions, where interduplex distances are dictated by overscreening the negative charges of the phosphate backbone. This subtle interplay between ionic strength and film structure is an important factor that should be considered when DNA films are investigated with use of cationic redox mediators. To circumvent some of these inherent difficulties, we have developed a method for monitoring the extent of surface coverage based on electrostatic repulsion between DNA and $Fe(CN)_6^{3-}$. The long-range interaction between the anionic redox probe and the film is insensitive to subtle morphological changes on the surface. The impedance response of $Fe(CN)_6^{3-}$ on DNA films therefore provides a reliable, although indirect, readout of the surface coverage, without the disadvantages encountered with $Ru(NH_3)_6^{3+}$ due to DNA packing.

Acknowledgment. We are grateful to the National Institutes of Health (GM61077) for their financial support of this research.

References and Notes

(1) Boon, E. M.; Ceres, D. M.; Drummond, T. G.; Hill, M. G.; Barton, J. K. *Nat. Biotechnol.* **2000**, *18*, 1096−1100.

(2) Ceres, D. M.; Barton, J. K. *J. Am. Chem. Soc.* **2003**, *125*, 14964−14965.

(3) Kelley, S. O.; Barton, J. K.; Jackson, N. M.; Hill, M. G. *Bioconj. Chem.* **1997**, *8*, 31−37.

(4) Kelley, S. O.; Boon, E. M.; Barton, J. K.; Jackson, N. M.; Hill, M. G. *Nucleic Acids Res.* **1999**, *27*, 4830−4837.

(5) Kelley, S. O.; Jackson, N. M.; Hill, M. G.; Barton, J. K. *Angew. Chem., Int. Ed.* **1999**, *38*, 941−945.

(6) Liu, T.; Barton, J. K. *J. Am. Chem. Soc.* **2005**, *127*, 10160−10161.

(7) Drummond, T. G.; Hill, M. G.; Barton, J. K. *J. Am. Chem. Soc.* **2004**, *126*, 15010−15011.

(8) Drummond, T. G.; Hill, M. G.; Barton, J. K. *Nat. Biotechnol.* **2003**, *21*, 1192−1199.

(9) Murphy, L. *Curr. Opin. Chem. Biol.* **2006**, *10*, 177−184.

(10) Boal, A. K.; Yavin, E.; Lukianova, O. A.; O'Shea, V. L.; David, S. S.; Barton, J. K. *Biochemistry* **2005**, *44*, 8397−8407.

(11) DeRosa, M. C.; Sancar, A.; Barton, J. K. *Proc. Natl. Acad. Sci. U.S.A.* **2005**, *102*, 10788−10792.

(12) Yavin, E.; Stemp, E. D. A.; O'Shea, V. L.; David, S. S.; Barton, J. K. *Proc. Natl. Acad. Sci. U.S.A.* **2006**, *103*, 3610−3614.

(13) *Electrochemistry of Nucleic Acids and Proteins*; Palecek, E., Scheller, F., Wang, J., Eds.; Elsevier Science: San Diego, CA, 2006; Vol. 1.

(14) Bloomfield, V. A. *Curr. Opin. Struct. Biol.* **1996**, *6*, 334−341.

(15) Bloomfield, V. A. *Biopolymers* **1997**, *44*, 269−282.

(16) Naegeli, R.; Redepenning, J.; Anson, F. C. *J. Phys. Chem.* **1986**, *90*, 6227−6232.

(17) Maniatis, T.; Venable, J. H.; Lerman, L. S. *J. Mol. Biol.* **1974**, *84*, 37-&.

(18) Manning, G. S. *Biophys. Chem.* **1978**, *9*, 65−70.

(19) Rill, R. L. *Proc. Natl. Acad. Sci. U.S.A.* **1986**, *83*, 342−346.

(20) Schellman, J. A.; Parthasarathy, N. *J. Mol. Biol.* **1984**, *175*, 313−329.

(21) Nguyen, T. T.; Grosberg, A. Y.; Shklovskii, B. I. *Phys. Rev. Lett.* **2000**, *85*, 1568−1571.

(22) Nguyen, T. T.; Grosberg, A. Y.; Shklovskii, B. I. *J. Chem. Phys.* **2000**, *113*, 1110−1125.

(23) Rau, D. C.; Parsegian, V. A. *Biophys. J.* **1992**, *61*, 246−259.

(24) Tanaka, M.; Grosberg, A. Y. *J. Chem. Phys.* **2001**, *115*, 567−574.

(25) Fang, Y.; Yang, J. *J. Phys. Chem. B* **1997**, *101*, 3453−3456.

(26) Koltover, I.; Wagner, K.; Safinya, C. R. *Proc. Natl. Acad. Sci. U.S.A.* **2000**, *97*, 14046−14051.

(27) Sun, X. G.; Cao, E. H.; Zhang, X. Y.; Liu, D. G.; Bai, C. L. *Inorg. Chem. Commun.* **2002**, *5*, 181−186.

(28) Steel, A. B.; Herne, T. M.; Tarlov, M. J. *Anal. Chem.* **1998**, *70*, 4670−4677.

(29) Boon, E. M.; Barton, J. K.; Bhagat, V.; Nersissian, M.; Wang, W.; Hill, M. G. *Langmuir* **2003**, *19*, 9255−9259.

(30) Su, L.; Sankar, C. G.; Sen, D.; Yu, H. Z. *Anal. Chem.* **2004**, *76*, 5953−5959.

(31) Yu, H. Z.; Luo, C. Y.; Sankar, C. G.; Sen, D. *Anal. Chem.* **2003**, *75*, 3902−3907.

(32) Bard, A. J.; Faulkner, L. R. *Electrochemical Methods, Fundamental and Applications*, 2nd ed.; John Wiley & Sons, Inc.: New York, 2001.